Physical Constraints for Beam Hardening Reduction using Polynomial Models

Tobias Würfl, Nicole Maaß, Frank Dennerlein, André Aichert and Andreas K. Maier

***Abstract*—Reconstruction algorithms for X-ray computed tomography typically assume a monochromatic X-ray beam and an energy independent attenuation coefficient of the materials along the ray. However, the attenuation coefficient of every material depends on energy, which leads to beam hardening artifacts in the reconstructed images. Recently reference-free algorithms for mono-material beam hardening artifact reduction based on the epipolar consistency condition have been introduced. These and reference-based algorithms apply a univariate polynomial model to the measured intensities prior to reconstruction. However consistency conditions reflect all sources of measurement errors. Other sources of inconsistency, notably truncation, may impact the model fitting and lead to low-quality reconstructions in spite of higher consistency. This work aims at avoiding such problems by imposing physically plausible constraints on the compensation functions. We introduce two necessary constraints on compensation functions namely monotonicity and convexity over the range of observations. Subsequently, we reformulate the optimization problem of polynomial models to yield only solutions obeying these constraints. Our formulation presents the advantage of being able to fit exactly all those functions, therefore not discarding plausible solutions. We show that this problem, despite being non-convex in the general case, is convex for the special case of polynomials of degree three. A measured data experiment is presented to demonstrate the effectiveness of our method.**

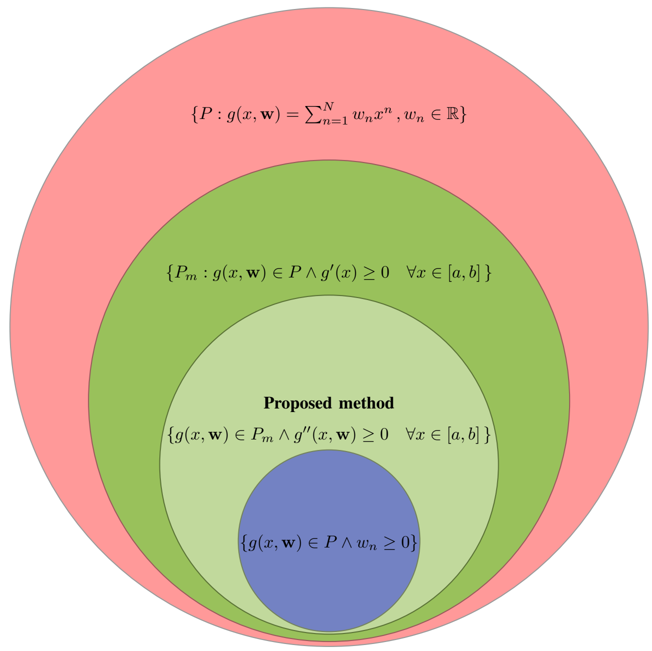

Figure 1: Venn diagramm of the different constraints. $[a, b]$ denotes the range of measured values of q.

I. Introduction

The combination of the polychromatic spectrum of X-ray tubes and the energy dependence of the linear attenuation coefficient causes a common problem in X-ray computed tomography known as beam hardening. This typically degrades image quality by introducing artifacts such as negative regions, cupping and streaks in reconstructions [1].

Conventionally the effect of beam hardening is compensated by a combination of software approaches which use reference measurements and methods optimizing the effective X-ray spectrum. An important distinction between software approaches is whether they assume a mono-material or a multi-material model. A computationally efficient mono-material method was presented by Kachelrieß et al. [2]. The approach introduces a polynomial compensation model and constructs a linear optimization problem to estimate its parameters using a reference measurement.

However, beam hardening introduces inconsistency in raw projection data which can be used to estimate parameters, even without any reference. New consistency conditions have been introduced for cone-beam data by Clackdoyle et al. [3], Lesaint et al. [4] and Debbeler et al. [5]. Aichert et al. provided an efficient flexible formulation of [5] in terms of epipolar geometry known as the epipolar consistency condition [6].

Recently, two reference-free beam hardening reduction algorithms based on the epipolar consistency condition and a univariate polynomal model have been presented by Abdurahman et al. [7] and Würfl et al. [8]. The approach by Würfl et al. uses the linearity of the Radon operator to speed up the algorithm significantly by reformulating the optimization problem on the Radon intermediate function. Additionally, the authors propose to improve robustness to other sources of inconsistency by requiring the coefficients of the polynomials to be non-negative. This non-negativity constraint on the coefficients is motivated by the observation that it is a sufficient but not necessary condition for a polynomial to be monotonously increasing.

We show that the requirement on the model functions to be monotonously increasing can be restricted further by considering the physics of X-ray attenuation by additionally requiring the functions to be convex.

This is implicitly satisfied by requiring non-negativity of

T. Würfl and A. K. Maier are with the Pattern Recognition Lab, Friedrich-Alexander-Universität Erlangen-Nürnberg (FAU), Erlangen, Germany.
N. Maaß and F. Dennerlein are with Siemens Healthcare GmbH, Erlangen, Germany.

the coefficients. However non-negativity of the coefficients is too restrictive in the sense that it prohibits many physically plausible solutions by not being a necessary condition. We illustrate this situation in Fig. 1. In this work, we present a new parametrization of polynomial functions which is necessary and sufficient for monotonously increasing polynomials with a monotonously increasing derivative over the range of interest. This is also depicted in Fig. 1 as the set of our proposed formulation is equal to the set of our proposed constraint. Despite the fact that the original optimization problem is convex the domain of the new parametrization is in general not convex which renders optimization non-convex. However we are able to show convexity for the special, practically relevant case of a polynomial of degree three.

II. Methodology

In section II-A we present physical constraints on our model function. We construct a parametrization of polynomials obeying these constraints in section II-B. Subsequently we discuss optimization of this new parametrization in section II-C.

A. Physical constraints on beam hardening reduction models

The log attenuation along a line in X-ray imaging is given as:

$$q(L) = -\ln \int S(L,E) e^{-\int_0^\infty \mu(E,\mathbf{s}+\lambda\mathbf{l})d\lambda} dE\,, \qquad (1)$$

where $S(E)$ is the normalized spectrum over energy E on the line of integration L parametrized as $\mathbf{s}+\lambda\mathbf{l}$. Here $\mathbf{s}$ denotes the source position and $\mathbf{l}$ the direction, while $\mu(E,\mathbf{r})$ denotes the spatial distribution at position $\mathbf{r}$ of the energy-dependent attenuation values along a line L. It is common to assume we can decompose the energy dependence from the spatial dependence. This allows us to reformulate Eq. (1) to:

$$q(\mathbf{r}) = -\ln \int S(E) e^{-p(\mathbf{r})\psi(E)} dE\,, \qquad (2)$$

where $p(\mathbf{r})$ denotes the mono-chromatic line-integral at position $\mathbf{r}$ at some effective energy, while $\psi(E)$ denotes the energy dependence. In order to obtain p from measurements q, the task is now to find the inverse to this function, which we will denote as f. This is depicted in Fig. 2.

Physically plausible model functions have to be monotonous and convex giving rise to the requirement:

$$f'(q) > 0 \quad \wedge \quad f''(q) > 0 \quad \forall\, q \in [0, q_{max}]\,. \qquad (3)$$

B. Parametrization

We introduce a new parametrization of our polynomial by extending a recently presented monotonic parametrization by Murray et al. [9]. The goal of their method is to fit a polynomial:

$$g(x,\mathbf{w}) = w_0 + w_1 x + \cdots + w_d x^d\,, \qquad (4)$$

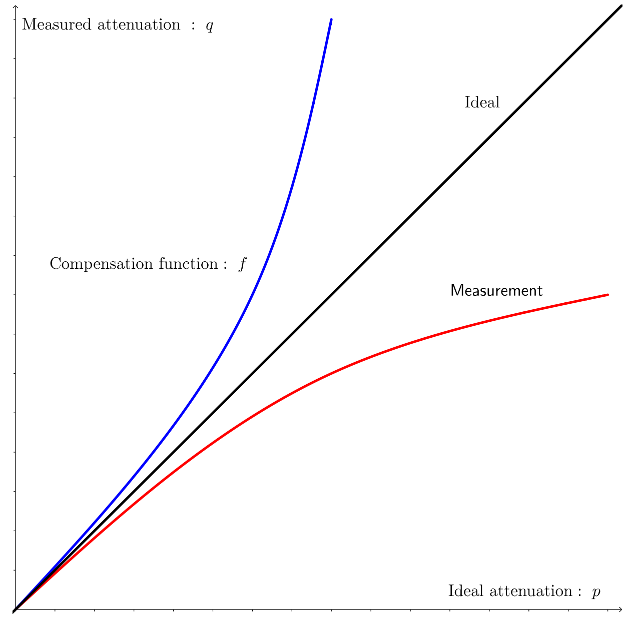

Figure 2: Illustration of the beam hardening effect.

where d denotes the degree of the polynomial, subject to the constraint of being monotonous over a range $[a,b]$. They use the fact that a polynomial of degree $d=2k$ is positive on $[a,b]$ if and only if it can be written as

$$\hat{g}(x,\hat{\mathbf{w}}_1,\hat{\mathbf{w}}_2) = \hat{g}_1(x,\hat{\mathbf{w}}_1)^2 + (x-a)(b-x)\hat{g}_2(x,\hat{\mathbf{w}}_2)^2\,, \qquad (5)$$

where k is a positive integer denoting the degrees of $\hat{g}_1$ and $\hat{g}_2$. If instead the degree is $d=2k+1$ we have

$$\hat{g}(x,\hat{\mathbf{w}}_1,\hat{\mathbf{w}}_2) = (x-a)\hat{g}_1(x,\hat{\mathbf{w}}_1)^2 + (b-x)\hat{g}_2(x,\hat{\mathbf{w}}_2)^2\,. \qquad (6)$$

Integration over this non-negative polynomial $\hat{g}(x,\hat{\mathbf{w}}_1,\hat{\mathbf{w}}_2)$ yields:

$$g(x,\hat{\mathbf{w}}) = \delta + \alpha \int_0^x \hat{g}(u,\hat{\mathbf{w}}_1,\hat{\mathbf{w}}_2)\mathrm{d}u\,. \qquad (7)$$

Note that all monotonic polynomials can be constructed in this manner. Their method interprets the parameters of polynomials $\hat{g}_1(x,\hat{\mathbf{w}}_1)$ and $\hat{g}_2(x,\hat{\mathbf{w}}_2)$ together with δ as a set of new parameters:

$$\hat{\mathbf{w}} = (\hat{\mathbf{w}}_1,\hat{\mathbf{w}}_2)\,,$$

making them a reparametrization of $g(x,\mathbf{w})$. By writing polynomial multiplication and addition as convolution and addition of coefficient vectors, an intermediate polynomial with coefficients $\tilde{w}$ representing a non-negative polynomial of degree $d-1$ from $\hat{\mathbf{w}}$ can be calculated. If we e.g. pick an uneven degree:

$$\tilde{\mathbf{w}} = (-a,1)^T * (\hat{\mathbf{w}}_1 * \hat{\mathbf{w}}_1) + (b,-1)^T * (\hat{\mathbf{w}}_2 * \hat{\mathbf{w}}_2)\,,$$

where $*$ denotes convolution. An integral over $\tilde{\mathbf{w}}$ can be computed according to:

$$\mathbf{w} = \left(\delta, \alpha\tilde{w}_0, \alpha\frac{\tilde{w}_1}{2}, \cdots, \alpha\frac{\tilde{w}_{d-1}}{d}\right)^T\,, \qquad (8)$$

where α controls if it is monotonously increasing or decreasing, i.e. $\alpha = \pm 1$.

We set $\alpha = 1$, since we only need increasing functions. Additionally we require the second derivative to be non-negative to satisfy Eq. (3). To this end we integrate a second time:

$$f(x) = \int_0^x \delta + \int_0^u \hat{g}(v, \hat{\mathbf{w}}) \mathrm{d}v \, \mathrm{d}u \,. \tag{9}$$

We set the constant coefficient arising from the second integration to zero because we expect zero attenuation for zero traversed material. This new parametrization restricts $f(x)$ to be convex but does not enforce monotonicity. Because the first integration yields a strictly positive polynomial over the range of interest we only need to constrain the parameter δ to be non-negative. This has a straightforward interpretation since δ is simply the slope at $x = 0$. A negative slope here cannot yield a sensible compensation polynomial. Because we started from a necessary and sufficient condition of non-negativity this new parametrization includes all polynomials which meet our physical requirements of Eq. (3).

C. Optimization of the new parametrization

The new parametrization can be incorporated into any scheme estimating a polynomial compensation model from measurements using a general non-linear optimizer. The parameters of the optimization are reparametrized and the cost function is evaluated using the intermediate weights.

An important distinction of optimization problems is whether they are convex and so any initial value will lead to the same unique global minimum. When applying the new parametrization this is in general not the case [9]. The problem stems from the fact that the domain of all monotonic polynomials $f(x)$ is not convex. Therefore, even though the unconstrained problem is convex, an optimizer can get stuck in local minima which are on the boundaries of the restricted domain.

In practice, a degree of $d = 3$ is often found to be sufficient for measured data. If we restrict our attention to this special case, we can investigate the function $\mathbf{m}_3(\delta, \hat{\mathbf{w}})$ which maps the optimization parameters $\delta, \hat{\mathbf{w}}_1, \hat{\mathbf{w}}_2$ to the parameters of our polynomial model. In this case $\hat{\mathbf{w}}_1 = \hat{w}_1$ and $\hat{\mathbf{w}}_2 = \hat{w}_2$ and thus:

$$\mathbf{w} = \mathbf{m}_3(\delta, \hat{\mathbf{w}}) = \begin{pmatrix} 0 \\ \delta \\ \frac{1}{2}\left(b\hat{w}_2^2 - a\hat{w}_1^2\right) \\ \frac{1}{6}\left(\hat{w}_1^2 - \hat{w}_2^2\right) \end{pmatrix} \,. \tag{10}$$

Since δ is constant, the shape of the domain depends only on the intermediate weights $\hat{w}_1$ and $\hat{w}_2$. We visualize this domain in Fig. 3. Examining the mapping in Eq. (10) we can state that the square-function maps every value in the four quadrants of $\hat{\mathbf{w}}$ to the same values in $\mathbf{w}$. In addition, we can determine that the boundaries of this domain are characterized by lines produced when $\hat{w}_1 = 0$ or $\hat{w}_2 = 0$ respectively. The lines are explicitly given as the left boundary: $\begin{pmatrix} \frac{1}{2} \\ -\frac{1}{6} \end{pmatrix} \hat{w}_2^2$ and

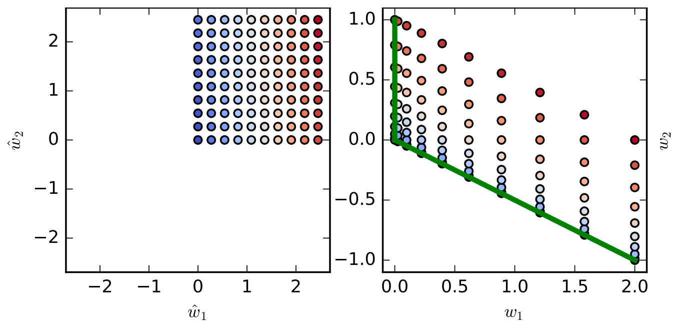

Figure 3: Visualization: $\mathbf{m}_3(\delta, \hat{\mathbf{w}})$ in relevant dimensions. The green lines form the treshold of the convex domain. $a = 0\,, b = \frac{4}{6}\,, \hat{w}_1 = \left[0, \sqrt{6}\right]\,, \hat{w}_2 = \left[0, \sqrt{6}\right]$

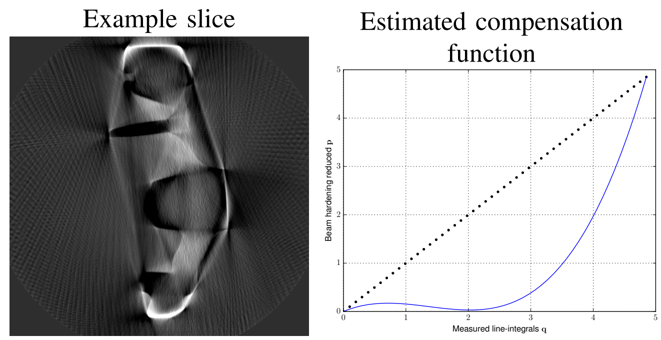

Figure 4: Results of the unconstrained ECC^2 algorithm using measured data of an aluminum part (cf. fig 5). The estimated compensation function shows undesired curvature and as a consequence, the reconstruction is flawed.

the lower boundary: $\begin{pmatrix} -\frac{a}{2} \\ \frac{1}{6} \end{pmatrix} \hat{w}_1^2$. Because the expression of the boundaries are lines which can also be seen graphically in Fig. 3 the domain of optimization is actually convex for the special case of a polynomial of degree three. This implies that the whole optimization problem is convex.

D. Application to the ECC^2 algorithm

The optimization problem for the reference-free beam hardening reduction algorithm of reference [8] is given as

$$\min \left(\|\mathbf{A}\mathbf{w}\|_2^2\right) \quad s.t. : \mathbf{w}^T\mathbf{b} = \beta; \quad w \geq 0 \quad \forall w \in \mathbf{w}\,, \tag{11}$$

Where $\mathbf{A}$ denotes a measurement matrix which is constructed using the epipolar consistency condition and $\mathbf{b}$ is a Vandermonde vector which fixes a point p to a value q to deal with the scale problem, inherent to the homogeneous least squares problem. We modify this algorithm using our new formulation to

$$\min \left(\|\mathbf{A}\,\mathbf{m}_d(\delta, \hat{\mathbf{w}})\,\|_2^2\right) \quad s.t. : \mathbf{m}_d(\delta, \hat{\mathbf{w}})^T\mathbf{b} = \beta\,, \delta > 0\,. \tag{12}$$

We can solve this problem using a standard solver for constrained convex optimization problems.

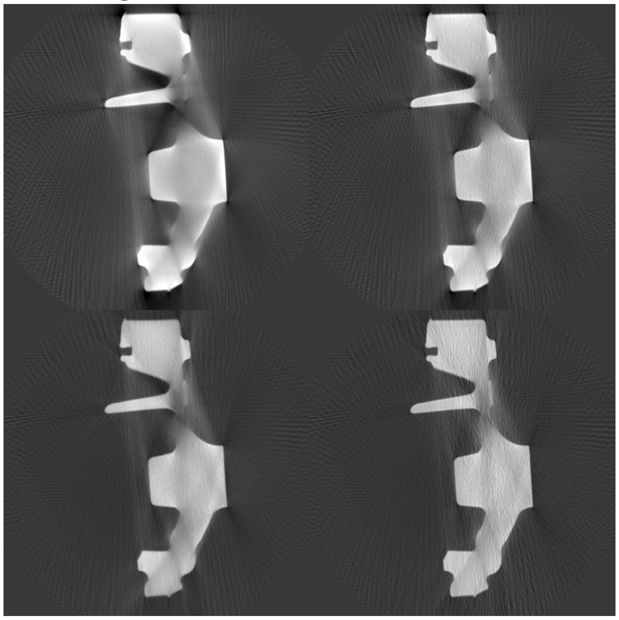

Figure 5: Comparison of the effect of scatter reduction on our modification of the ECC^2 algorithm. Because the ECC^2 algorithm does not preserve scale, we normalized every image to a mean of one (Grayscale window: C/W = 0.53/1.91).

III. Experiments

We present an experiment demonstrating our new method on a measured dataset of an aluminum object additionally affected by scatter.

The dataset shows severe scatter artifacts in addition to beam hardening. This is reflected in additional inconsistency. In Fig. 4 we present the result of the ECC^2 algorithm without a constraint on the polynomial:

The image-quality is severely impaired. The reason can be observed from the estimated polynomial which is neither monotonous nor convex.

We next compare the application of our proposed method to both the original data and scatter reduced data. The scatter reduction was performed using a beam stop array method. The results are presented in Fig. 5.

In Fig. 5 we demonstrate, that our proposed constraint makes the algorithm robust to additional sources of inconsistency. In addition we can see that the beam hardening related artifacts are removed in both cases, while the additional removal of scatter provides increased image quality independent of this.

IV. Conclusion and Outlook

We have shown a new parametrization of polynomial models which restricts the space of functions to a physically plausible subset. Specifically we improve previous approaches by precisely specifying the necessary conditions on these functions and providing a method restricting the results to all those functions which obey them. This can directly be used to improve a number of algorithms relying on such a model. Especially reference-free algorithms profit from our new formulation, as their functions of merit may actually reflect any other imaging problem in addition to beam hardening. We applied our method to the ECC^2 algorithm of Würfl et al.[8] and showed the effectiveness of our method in dealing with severe scatter conditions. Our algorithm is more complicated in terms of implementation and looses the advantage of presenting a convex optimization problem, if polynomials higher than degree three are considered. However we have not found this to be a practical limitation.

We will extend the physical constraints to multi-material methods in future research using similar techniques. This is more complicated since there is no unique definition of a convex functional of two coupled variables. We expect multi-material methods to benefit even more from such techniques because the problem has more degrees of freedom.

Additionally we are interested in applying our method to simultaneous multi-dimensional optimization of reference-free geometric and physical compensation methods promising to provide improved results for all those methods.

Acknowledgment

A. Aichert is supported by the German Research Foundation; DFG MA 4898/3-1.

Disclaimer

The concepts and information presented in this paper are based on research and are not commercially available.

References

[1] T. M. Buzug, Ed., *Computed Tomography*. Springer, 2008.
[2] M. Kachelrieß, K. Sourbelle, and W. A. Kalender, "Empirical cupping correction: A first-order raw data precorrection for cone-beam computed tomography," *Medical Physics*, vol. 33, no. 5, pp. 1269–1274, 2006.
[3] R. Clackdoyle, L. Desbat, J. Lesaint, and S. Rit, "Data consistency conditions for cone-beam projections on a circular trajectory," *IEEE Signal Processing Letters*, vol. 23, no. 12, pp. 1746–1750, 2016.
[4] J. Lesaint, R. Clackdoyle, S. Rit, and L. Desbat, "Two cone-beam consistency conditions for a circular trajectory," in *Proc. 4th Int. Conf. Image Formation X-Ray Comput. Tomography*, 2016, pp. 431–434.
[5] C. Debbeler, N. Maass, M. Elter, F. Dennerlein, and T. M. Buzug, "A new CT rawdata redundancy measure applied to automated misalignment correction," in *Fully Three-Dimensional Image Reconstruction in Radiology and Nuclear Medicine*, 2013, pp. 264–267.
[6] A. Aichert, M. Berger, J. Wang, N. Maass, A. Doerfler, J. Hornegger, and A. K. Maier, "Epipolar consistency in transmission imaging," *IEEE Transactions on Medical Imaging*, vol. 34, no. 11, pp. 2205–2219, 2015.
[7] S. Abdurahman, R. Frysch, R. Bismarck, M. Friebe, and G. Rose, "Calibration free beam hardening correction using Grangeat-based consistency measure," in *Nuclear Science Symposium and Medical Imaging Conference*, 2016.
[8] T. Würfl, N. Maass, F. Dennerlein, X. Huang, and A. Maier, "Epipolar Consistency Guided Beam Hardening Reduction - ECC^2," in *Fully Three-Dimensional Image Reconstruction in Radiology and Nuclear Medicine*, 2017, pp. 181–185.
[9] K. Murray, S. Müller, and B. Turlach, "Fast and flexible methods for monotone polynomial fitting," *Journal of Statistical Computation and Simulation*, vol. 86, no. 15, pp. 2946–2966, 2016.